Shimizu, B., Asai, M., Hieda, H., Miyaki, M., and Okazaki, H. (1965), *Chem. Pharm. Bull. 13*, 616.
Shimizu, B., Saito, A., Nishimura, T., and Miyaki, M. (1967), *Chem. Pharm. Bull. 15*, 2011.
Šmejkal, J., and Šorm, F. (1964), *Collect. Czech. Chem. Commun. 29*, 2809.
Staněk, J., Černý, M., Kocourek, J., and Pacák, J. (1963), The Monosaccharides, Translated by Mayer, K., New York, N. Y., Academic, p 77.
Stevens, C. L., and Felsenfeld, G. (1964), *Biopolymers 2*, 293.
Sulston, J., Lorhmann, R., Orgel, L. E., and Miles, H. T. (1968), *Proc. Nat. Acad. Sci. U. S. 59*, 726.
Ts'o, P. O. P., Kondo, N. S., Schweizer, M. P., and Hollis, D. P. (1969), *Biochemistry 8*, 997.
Wolfe, F. H., Oikawa, K., and Kay, C. M. (1969), *Can. J. Biochem. 47*, 977.
Wu, A. F., and Chargaff, E. (1969), *Proc. Nat. Acad. Sci. U. S. 63*, 1222.
Yamazaki, A., Kumashiro, I., and Takenishi, T. (1968), *Chem. Pharm. Bull. 16*, 338.
Yoshikawa, M., Kato, T., and Takenishi, T. (1967), *Tetrahedron Lett.*, 5065.

Conformational Studies on Transfer Ribonucleic Acid. Fluorescence Lifetime and Nanosecond Depolarization Measurements on Bound Ethidium Bromide*

Terence Tao,† James H. Nelson, and Charles R. Cantor‡

ABSTRACT: Ethidium bromide has been used as a fluorescent probe of the conformation of unfractionated yeast tRNA and purified yeast $tRNA^{Phe}$. A variety of types of data suggest that the dye binds by intercalation and that there is one principal binding site for the dye on $tRNA^{Phe}$ in the absence of magnesium. Time-dependent fluorescence depolarization measurements show that in the presence of magnesium both tRNA samples behave as a prolate ellipsoid with an axial ratio of 2.0 to 3.0. This is consistent with previous estimates of the size and shape of tRNA. In the absence of magnesium the unfractionated tRNA sample becomes considerably elongated and resembles a prolate ellipsoid with an axial ratio of 4.6. This change is accompanied by a shift in the circular dichroism spectrum indicative of disruption of base pairs. No such changes in overall conformation are observed for yeast $tRNA^{Phe}$. Nevertheless there is evidence for small changes in this purified sample as a function of magnesium concentration. There are revealed by studies of the quenching of the fluorescence of the Y base of $tRNA^{Phe}$ by ethidium bromide. Addition of ethidium bromide has no effect on the lifetime of Y either in the absence or presence of magnesium.

However, studies of static fluorescence show that the Y base is drastically quenched by ethidium bromide in the absence of magnesium. Only slight quenching occurs if magnesium is present. These results suggest that ethidium binds very close to Y if no magnesium is present, and very far away if there is magnesium in solution.

Applications of fluorescence lifetime and nanosecond depolarization techniques to the study of protein conformations have been very successful in recent years. These studies can yield such valuable information as the polarity at specific regions of a macromolecule, the rotational relaxation times and thus size and shape parameters (Wahl and Timasheff, 1969; Tao, 1969), and distances between chromophores attached to the macromolecule (Stryer, 1968). Although steady-state fluorescence measurements have long been used for the same type of studies, their interpretation is less direct than the time-resolved methods, and often requires tedious concentration and viscosity-dependent experimentation.

This paper describes conformational studies on unfractionated yeast tRNA and yeast $tRNA^{Phe}$ following much the same lines of approach as those described above. The conformation of tRNA is of much interest in view of the dependence of its biological activity on its structural integrity (Adams *et al.*, 1967; Lindahl *et al.*, 1966). Much information already exists on possible secondary structures (Madison, 1968; Cramer *et al.*, 1968; Cantor *et al.*, 1966) and overall size and shape of tRNA (Lake and Beeman, 1968; Krigbaum and Godwin, 1968; Adams *et al.*, 1967; Ninio *et al.*, 1969; Beardsley and Cantor, 1970). This can greatly assist the interpretation of nanosecond depolarization results. Previous studies have suggested that tRNA may resemble a prolate ellipsoid. This offers the possibility of observing more complex rotational relaxation behavior than has been found for typical globular proteins. Most tRNAs are known to undergo structural changes which are dependent on the magnesium

* From the Departments of Chemistry and Biological Sciences, Columbia University, New York, New York 10027. *Received December 12, 1969.* Supported by grants from the National Institutes of Health (GM 14825 to C. R. C., and CA 07712 to Professor Richard Bersohn).

† Present address: Department of Molecular Biophysics and Biochemistry, Yale University.

‡ Alfred P. Sloan Fellow.

TABLE I: Description of tRNA Samples Used.

Designation of Sample	Material	Concentration[a]		Concn of Mg^{2+}	Concn of EB	tRNA:EB
		mg/ml	mole/l.	mole/l.	mole/l.	
A	Unfractionated yeast tRNA	2.6	1.0×10^{-4}	0.04	5×10^{-5}	2.0
B	Unfractionated yeast tRNA	1.5	5.7×10^{-5}	0.003	5×10^{-5}	1.1
C	Unfractionated yeast tRNA	2.6	1.0×10^{-4}	0.0[b]	5×10^{-5}	2.0
D	Yeast $tRNA^{Phe}$	1.8	6.8×10^{-5}	0.0026	6.4×10^{-5}	1.1
E	Yeast $tRNA^{Phe}$	1.8	6.8×10^{-5}	0.0[b]	5.8×10^{-5}	1.2

[a] Molecular weight of bulk yeast tRNA was taken to be 26,400 g/mole (Lindahl *et al.*, 1965). Molecular weight of 24,000 g/mole was estimated from the published nucleic acid sequence of $tRNA^{Phe}$ (RajBhandary *et al.*, 1967). [b] Contains 0.001 M NaCl instead. See text for details.

ion concentration (Penniston and Doty, 1963; Adams *et al.*, 1967; Reeves *et al.*, 1970). These transitions can be conveniently followed by circular dichroism measurements. If fluorescence properties are also affected more detailed information about the structural changes could be derived. Finally, purified yeast $tRNA^{Phe}$ contains a naturally fluorescent nucleotide, Y, located adjacent to the anticodon as part of the sequence GAAYAψ (RajBhandary *et al.*, 1967; Thiebe and Zachau, 1968). Apart from the interest in this fluorescence for its own sake, this nucleotide can be used as the donor for energy-transfer measurements (Beardsley and Cantor, 1970).

Unlike proteins, however, most tRNAs do not possess naturally fluorescent groups of appreciable yield or lifetime. We have used the dye ethidium bromide (2,7-diamino-9-phenyl-10-ethylphenanthridinium bromide)[1] as an extrinsic fluorescence probe. This choice was mediated by several circumstances: the fluorescence yield (LePecq and Paoletti, 1967) and lifetime of EB is dramatically enhanced when bound by double-stranded nucleic acids. Furthermore, EB is believed to intercalate between base pairs (Fuller and Waring, 1967). Thus EB can be used as a probe for helical regions in the clover leaf model for tRNAs, much as ANS has been widely used as a fluorescence probe for hydrophobic regions of proteins (Weber and Laurence, 1954). Like ANS, EB enjoys the highly attractive feature that bound dye contributes virtually all of the total fluorescence and therefore one need not make corrections for free dye. In addition, because EB binds by intercalation, the bound dye is likely to remain on the macromolecule within the lifetime of the fluorescent state (Li and Crothers, 1969), likely to have a fixed orientation with respect to the macromolecule, and not likely to have rotational freedom. Thus our nanosecond depolarization measurements are free from such artifacts as contributions from unbound dye, and rotational movement of the fluorescence label itself. This is in contrast to earlier studies which used covalently attached acriflavin as a fluorescent label (Millar and Steiner, 1966; Churchich, 1963). The homogeneity of dye orientation also assures us of homogeneous rotational relaxation behavior, rather than a composite of relaxation characteristics arising from each dye orientation (see analysis given later in the text). Finally, the visible absorption of EB overlaps with the emission of the Y group sufficiently well to allow its use as an energy acceptor (Stryer and Haugland, 1967). The activity of $tRNA^{Phe}$ as judged by the ability to load phenylalanine, is unaffected by the presence of EB.

[1] Hereafter abbreviated as EB. The other abbreviation used in this paper is: ANS, 1-anilino-8-naphthalenesulfonate.

Materials

Ethidium bromide was a gift from the Boots Pure Drug Co. Ltd., Nottingham, England. Unfractionated yeast tRNA was purchased from Schwartz BioResearch, Inc. Purified yeast $tRNA^{Phe}$ was purchased from Boehringer Mannheim. This commercial product, as assayed in our laboratory, loaded 1200 $\mu\mu$moles of [^{14}C]phenylalanine/A_{260} unit, indicating a purity of 68%. The concentrations of the materials in various samples are given in Table I. All solutions were buffered with 0.02 M Tris-HCl (pH 8.0). Samples A, B, and D contained sufficient magnesium to allow at least one Mg^{2+} ion in solution for every two phosphate groups on the tRNA backbone. For the depolarization experiments the molar concentrations of EB were always sufficiently less than that of the tRNA, that it was unlikely for two dye labels to be on the same macromolecule. Sample C (unfractionated tRNA, no Mg^{2+}) was prepared by dissolving the tRNA in a solvent containing 0.001 M NaCl in addition to the Tris-HCl buffer. This solution was then heated at 60° for 5 min before allowing it to cool to room temperature in a period of 1.5 hr. Circular dichroism studies indicated that this treatment caused considerable loss of tRNA secondary structure. For sample E ($tRNA^{Phe}$, no Mg^{2+}) it was feared at first that there might be sufficient magnesium ions in the commercial product to keep the material in a native conformation. Exhaustive dialysis (Reeves *et al.*, 1970), as well as heating at 60°, was carried out to remove the residual magnesium. The experimental results were unaffected by these treatments.

Methods

Circular dichroism spectra were routinely obtained on a Cary 60 spectrometer using the Cary 6001 circular dichroism attachment. All instrument parameters and data reduction have been described previously (Cantor *et al.*, 1969). Circular

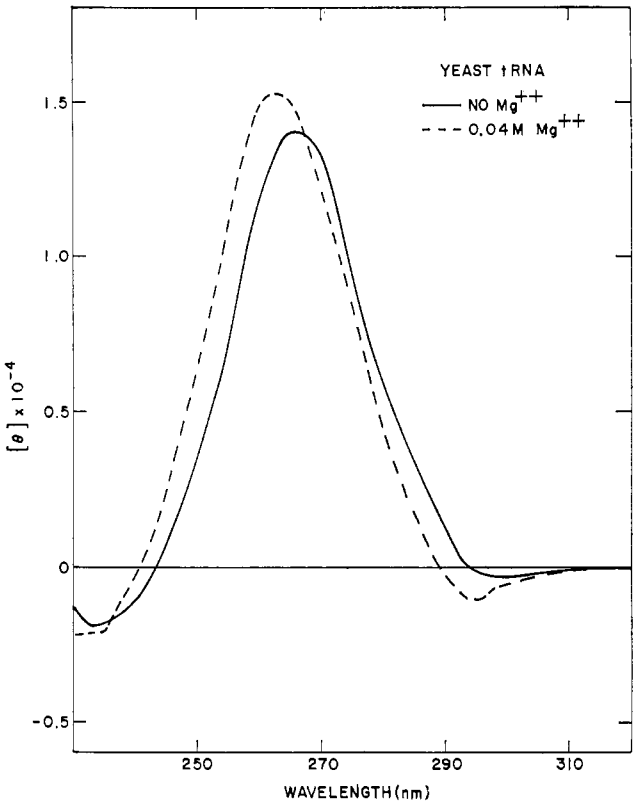

FIGURE 1: Effect of magnesium ion on the circular dichroism of unfractionated yeast tRNA.

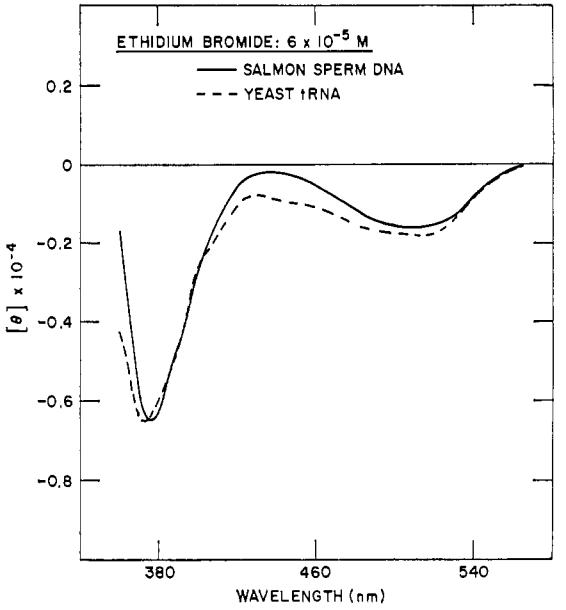

FIGURE 2: Circular dichroism of ethidium bromide bound to nucleic acids. In each case, the dye was saturated with excess nucleic acid.

dichroism measurements were made on the exact same solutions used for fluorescence studies by employing 0.1-mm cells.

Steady-State Fluorescence Measurements. Fluorescence intensity measurements with continuous excitation were routinely carried out on a laboratory built fluorometer (C. K. Luk, manuscript in preparation). The instrument employs Jarrell-Ash quarter-meter monochromators, chopped excitation and emission beams at right angles, and phase-sensitive amplification. For measurements associated with the binding and quenching studies, 1-mm path-length cells were used to ensure uniform optical densities in each sample. The cells were aligned at 45° to the excitation beam. Less scattering was present when the emission was detected from the *backside* of the cell.

Fluorescence Lifetime Measurements. The single photon-counting apparatus for the detection of emission events in the nanosecond region has been described (Tao, 1969). In most measurements a monochromator was used to select the emission wavelengths, and appropriate Corning glass filters were used to select the excitation wavelengths. For the depolarization measurements, however, the red EB emission was found to be almost completely depolarized when activated by ultraviolet light of wavelengths shorter than 400 nm. In order to excite only the visible band, a combination of Corning 7-59 and 3-75 filters was employed on the excitation beam. A Corning 2-63 filter selected only the red emission of EB. A detailed discussion of the fitting procedures used in analysis of the data is given in the accompanying manuscript (Beardsley *et al.*, 1970).

Nanosecond Depolarization Measurements. The detailed procedures for measuring the decay of the fluorescence polarization anisotropy $r(t)$ have been described previously (Tao, 1969). The experimental curves $I_{\parallel}(t)$ and $I_{\perp}(t)$ are first determined. The depolarization curves $d(t) = I_{\parallel}(t) - I_{\perp}(t)$ are constructed. The natural decay of the fluorescence $s(t) = I_{\parallel}(t) + 2I_{\perp}(t)$ is determined independently. This is achieved by orienting the polarizer such that the electric vector of the excitation beam makes an angle of 54.7° to the normal axis of the experimental plane. Meanwhile, the analyzer is oriented to pass only emission polarized parallel to this vertical axis. The experimental $s(t)$ curves were fitted with either one or two exponentials. The anisotropy curves $r(t) = d(t)/s(t)$ were obtained by point by point division.

It should be noted that when the data are treated in such a manner there is a certain amount of systematic error that tends to lengthen the relaxation times so obtained. This is due to the finite width of the excitation pulse. When the decay process is long compared with the decay of the excitation pulse, this error may be ignored. For the excitation source that was used, the error for a 25-nsec relaxation time is about 1 nsec which is comparable with the random errors incurred during these measurements.

Results and Discussion

Circular Dichroism of tRNA. Circular dichroism spectra were used to monitor the magnesium-dependent conformational changes of tRNA. The circular dichroism spectra of unfractionated yeast tRNA in the presence and absence of added magnesium were markedly different (see Figure 1). As magnesium was removed, there was a decrease in ellipticity, a red shift of the peak, and the small negative peak at 295 nm almost completely disappeared. The circular dichroism results for unfractionated yeast tRNA are typical of those tRNAs that undergo a transition with magnesium

TABLE II: Fluorescence Decay Parameters of Nucleic Acid Bound EB.[a]

Sample	a'	τ' (nsec)	a''	τ'' (nsec)
A, bulk, 0.04 M Mg^{2+}	0.10	14	0.90	28.0
B, bulk, 0.003 M Mg^{2+}	0.15	13	0.85	27.6
C, bulk, no Mg^{2+}	0.07	12	0.93	27.6
D, Phe, 0.0026 M Mg^{2+}	0.15	11	0.85	25.6
E, Phe, no Mg^{2+}	0.00		1.00	26.2
Calf thymus DNA	0.00		1.00	23.3

[a] $s(t) = a'e^{-t/\tau'} + a''e^{-t/\tau''}; a' + a'' = 1.$

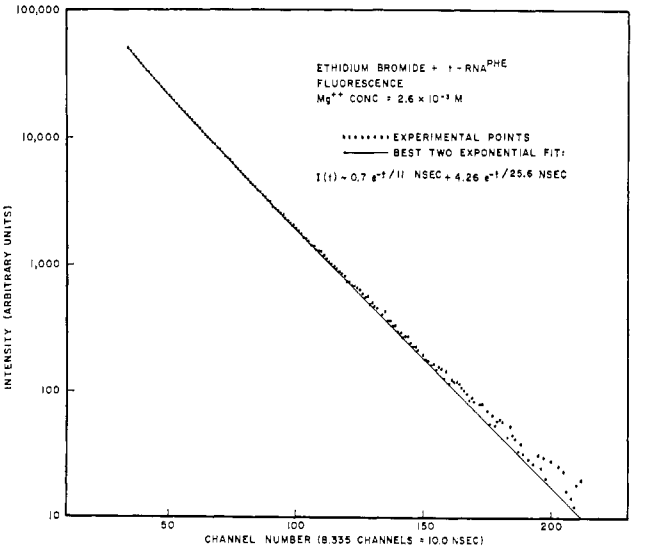

FIGURE 3: Fluorescence decay of ethidium bromide bound to yeast $tRNA^{Phe}$ in the presence of magnesium. The details of the sample used are described in Table I.

ion concentration. The decrease in ellipticity and shift towards longer wavelength as magnesium is removed are indicative that hydrogen bonds have been broken in the tertiary or secondary structure (Adams *et al.*, 1967; Reeves *et al.*, 1970). In contrast, the shape of the circular dichroism spectrum of $tRNA^{Phe}$ was essentially independent of magnesium ion under the conditions used in this study. Some small decrease in magnitude of the principle 267-nm positive cotton effect was observed as magnesium was removed but no red shift of this band was noticed (Beardsley *et al.*, 1970). This type of spectral change is most likely associated with the disruption of a small number of base pairs to produce *unstacked* residues. Apparently, purified yeast $tRNA^{Phe}$ is more resistant to denaturation than most tRNAs. The shape of its circular dichroism spectra is virtually independent of magnesium ion concentration. Thus, it was of considerable interest to compare this species with unfractionated tRNA in our fluorescence studies.

Binding of Ethidium Bromide to tRNA. Before EB could be used as a fluorescent probe it was first necessary to characterize its binding with the tRNA. The circular dichroism spectrum of bound ethidium bromide was measured on samples of dye saturated with either excess DNA or excess unfractionated yeast tRNA. These two spectra are compared in Figure 2. Since free ethidium bromide is optically inactive, the circular dichroism spectrum of the bound dye reflects the asymmetric environment of the binding site. The extreme similarity of the circular dichroism spectra shown in Figure 2 is evidence that the binding site for EB on tRNA is virtually the same as that on DNA.

Like double-stranded DNA and RNA (LePecq and Paoletti, 1967), tRNA enhanced the fluorescence intensity of bound EB some 20-fold. When tRNA was added, the fluorescence lifetime of EB lengthened from less than 1.5 nsec to about 26 nsec. For most samples, however, the fluorescence decay curves contained a small proportion of a short lifetime component in addition to the main long-lived component. These curves could be fitted with an iterative least-squares program. A typical fit is shown in Figure 3. The decay parameters are tabulated in Table II. Note that the amount of the short component is reduced for bulk tRNA without magnesium, and is undetectable for the sample of $tRNA^{Phe}$ without magnesium. The fluorescence of EB bound to calf thymus DNA also decayed with a single exponential of lifetime, 23.3 nsec. It is well established that EB intercalates between base pairs of double-stranded nucleic acids (Fuller and Waring, 1964). The properties of tRNA-bound EB and double-strand DNA-bound EB are so similar (circular dichroism spectra, enhancement of fluorescence yield, fluorescence decay characteristics, etc.) that EB is very certainly intercalated at helical regions of tRNA. Similar conclusions have recently been reached by Bittmann using a variety of other physical techniques (1969).

To obtain some indication of the degree of EB binding, the static fluorescence was measured as a function of the dye to tRNA ratio. These results are shown in Figure 4. Both in the absence of magnesium (Figure 4a) and in the presence of magnesium (Figure 4b) the EB fluorescence rose sharply at low dye to $tRNA^{Phe}$ concentrations, but began to flatten out at a dye to tRNA concentration of less than 2:1. Most of the increase in fluorescence above this ratio is due to free dye or weakly fluorescent dye in secondary binding sites (LePecq and Paoletti, 1967). (Note that the intensities in the two figures cannot be compared directly with each other. Only relative yields were measured.) This suggests that at low dye to tRNA ratios there may be as little as only one available binding site. Dyes bound to this site have strongly enhanced fluorescence.

For the sample without magnesium, the enhancement curve was extended to higher dye concentrations. From the known fluorescence of free dye (LePecq and Paoletti, 1967) and an estimate of the relative yield of bound dye, the relative amounts of both could be calculated given the total amount of dye added to the solutions. A Scatchard plot was made from the data. This is shown in Figure 5. This plot shows an initial sharp linear region followed by curvature and a drastic decrease in slope at high EB to $tRNA^{Phe}$ ratios. The intercept of a linear extrapolation of the first part of the plot demonstrates that there is one strong binding site for EB under these conditions. This has a binding constant

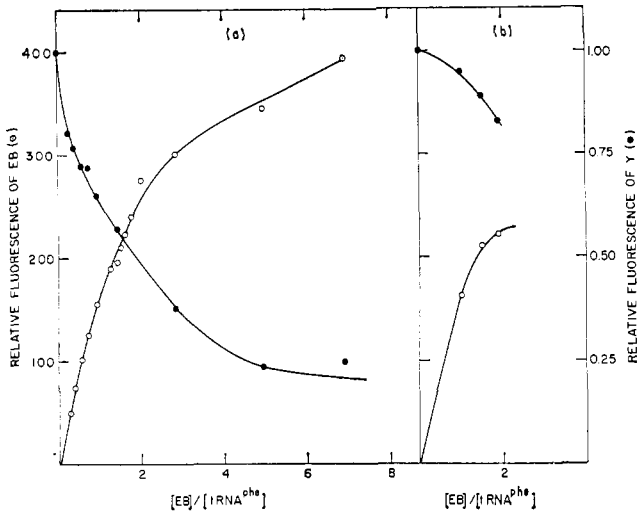

FIGURE 4: Relative fluorescence of ethidium bromide (⊙—⊙) (λ_{ex} = 520 nm; λ_{em} = 581 nm) and the fluorescent nucleotide, Y, of $tRNA^{Phe}$ (λ_{ex} = 320 mμ; λ_{em} = 430 mμ) as a function of [EB]/[tRNA]. The concentration of $tRNA^{Phe}$ is 1.25 × 10^{-5} M. The fluorescence of Y is defined to be 1.0 in the absence of ethidium bromide. (a) Data obtained in the absence of magnesium and (b) data obtained in 0.0026 M magnesium ion.

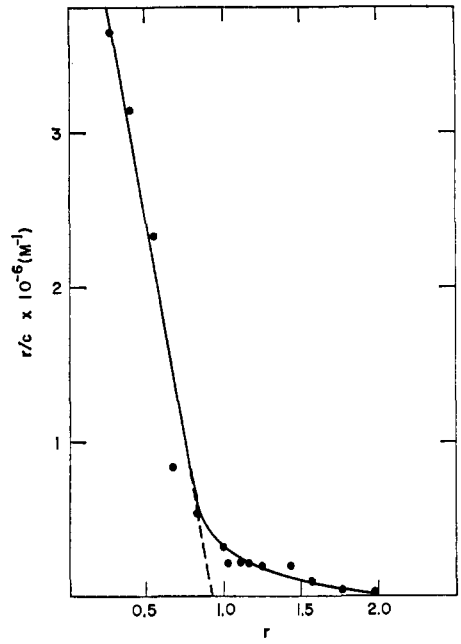

FIGURE 5: Scatchard plot of the data of Figure 4a. The binding constant derived from this plot is 6 × 10^6 M^{-1}. The curvature in the plot may be due to binding to secondary sites which have lower affinity for the dye. In this figure r is the number of dye molecules bound per $tRNA^{Phe}$ and c is the concentration of free dye.

of 6 × 10^6 M^{-1}. The curvature and subsequently gently sloping results show the existence of other much weaker binding sites. The conclusion that there is only one strong binding site on $tRNA^{Phe}$ in the absence of added magnesium is further substantiated by the finding that the decay of EB fluorescence is a simple exponential when bound to tRNA in the absence of magnesium.

Under favorable conditions, we should have been able to obtain more detailed binding data for $tRNA^{Phe}$ in the presence of magnesium. However, the presence of more than one exponential in the fluorescence decay spectra indicated that there must be more than one class of binding sites. This probably can best be understood in terms of the primary and secondary modes of binding that LePecq and Paoletti (1967) discussed. To sort out the precise occupations of different classes of sites would require an extensive study. Due to the scarcity of material, however, this has not been done.

The fact that there was only one strong binding site for EB on $tRNA^{Phe}$ at low magnesium ion concentration was at first quite surprising. Much higher numbers of binding sites per base pair are found, for example, in DNA (LePecq and Paoletti, 1967). Our result can, however, be rationalized in the following simple way. When EB binds, the double helix must increase in length to accommodate the dye. But such a process is energetically much less favorable if that helix is part of an ordered tertiary structure. Hence we may be observing binding only to those helices which protrude from the bulk of the tertiary structure.

Proximity of Bound EB to the Y Base of $tRNA^{Phe}$. Ethidium bromide should be able to quench the fluorescence of the Y base of $tRNA^{Phe}$ by singlet-singlet energy transfer. The theory of this phenomenon has been worked out in detail by Förster and many aspects of the theory have been verified by Stryer and his collaborators (Stryer and Haugland, 1967; Haugland *et al.*, 1969). The relative efficiency of energy transfer is dependent on the sixth power of the distance between donor (Y) and acceptor (ethidium bromide). The efficiency of transfer is simply one minus the fraction of the donor fluorescence that is quenched. An important parameter which characterizes the system is R_0, the donor–acceptor distance at which energy transfer is half-efficient, and the donor is 50% quenched. For Y and ethidium bromide this is calculated to be 23 Å. The method of calculation has been described in detail elsewhere (Beardsley and Cantor, 1970).

The fluorescence of the Y nucleotide contained in yeast $tRNA^{Phe}$ can be excited in the range of 300–340 nm. It emits at 440 nm, where there is no EB emission. Thus one can easily follow the quenching of Y by the bound dye. The fluorescence of Y as a function of the amount of EB added is shown in Figure 4. The Y fluorescence was normalized such that the intensities at zero dye concentration was 100% in both samples. This was necessary because the fluorescence of Y is strongly dependent on magnesium concentration (Beardsley *et al.*, 1970). There were striking differences in the quenching curves between the sample with magnesium and without magnesium. Addition of EB to magnesium-free tRNA caused severe quenching of Y. This quenching closely paralleled the extent of EB binding as exhibited by the dye fluorescence (Figure 4a). In contrast, the quantum efficiency of Y in the presence of magnesium was only slightly affected by the addition of dye. The small amount of quenching that is observed did not follow the binding of fluorescent EB (Figure 4b). Note from Figure 4a that even at high dye to $tRNA^{Phe}$ concentrations quenching was not complete.

To obtain an independent measurement on the extent

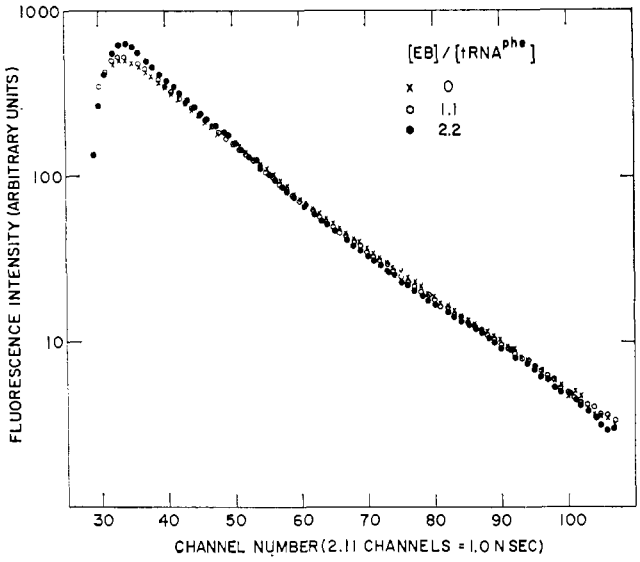

FIGURE 6: Fluorescence decay of the Y base of $tRNA^{Phe}$ in the presence of magnesium as a function of the amount of ethidium bromide added to the solution. All of the curves have been normalized to have the same area under the curve. The magnesium concentration is 0.0026 M.

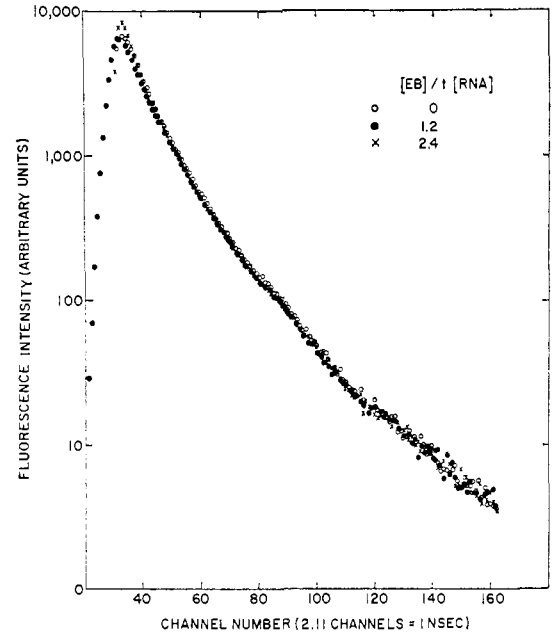

FIGURE 7: Same as Figure 6 except that data were obtained in the absence of magnesium ion.

that Y was quenched by EB, the fluorescence decay of Y was measured as a function of the amount of added dye. These results are shown in Figures 6 and 7. In the presence of magnesium, the decay of the Y fluorescence was nearly exponential with a lifetime of 6.3 nsec. The pulse width of the exciting light is considerably shorter than this lifetime. See, for example, the representative pulse shape shown in Figure 5 of the accompanying manuscript (Beardsley *et al.*, 1970). Thus, we should have been able to observe quenching of Y by a decrease in its fluorescence lifetime. In the absence of magnesium the lifetime of Y is 4 nsec, somewhat shorter than in magnesium-containing samples. This decrease is discussed in detail elsewhere (Beardsley *et al.*, 1970). Again, however, the lifetime of Y is long enough such that quenching should be experimentally visible as a decrease in lifetime.

The striking result shown in Figures 6 and 7 is that, within our experimental error, the decay of Y fluorescence was clearly independent of the amount of EB added whether in the presence or absence of magnesium. This can only be explained by an essentially all-or-none quenching process. In the absence of magnesium the observed static fluorescence is drastically quenched by EB. The lifetime is unchanged because the only Y groups still showing appreciable fluorescence are those on tRNAs which contain no bound EB. Thus the efficiency of quenching is close to 100%, which means that the distance between Y and the bound EB is considerably less than R_0, 23 Å. Since the Y base is on the anticodon loop, and the double-helical region adjacent to this loop is five base pairs long (~15 Å), it seems quite likely that the bound dye is somewhere in this region. A precise estimate of the distance is impossible since at high quenching efficiencies the results are almost independent of distance.

For the explanation given above to be completely consistent, we should have observed complete quenching of the static fluorescence of Y as the dye to tRNA ratio was increased. That this is not found may be due to the presence of some $tRNA^{Phe}$ in a conformation incapable of binding tRNA. The results presented in the accompanying manuscript indicate that magnesium causes a conformational change in $tRNA^{Phe}$ which takes place over a very broad range of divalent ion concentrations. In none of the experiments reported here can we guarantee that all of the molecules were in one form or the other.

If magnesium is present, much less quenching of the static fluorescence of Y is observed as EB is added to $tRNA^{Phe}$ Again, no change in fluorescence lifetime is observed. A detailed interpretation of these results would require much more data than thus far obtained owing to the presence of more than one type of binding site for the dye. However, the highly diminished quenching almost certainly means that the principal binding site for EB which dominated the binding in the absence of Mg^{2+} is not a strong binding site if Mg^{2+} is present. Since EB still can bind to $tRNA^{Phe}$ in magnesium, the binding must occur at another site or sites, and these are not located close to Y. These results are summarized in the highly schematic picture shown in Figure 8.

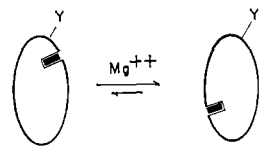

FIGURE 8: Schematic drawing of the effect of magnesium on the binding characteristics of ethidium bromide to $tRNA^{Phe}$. It is probable that in the experiments described herein, both forms were present to some extent under all conditions. The solid rectangle shows EB bound to the principal binding site.

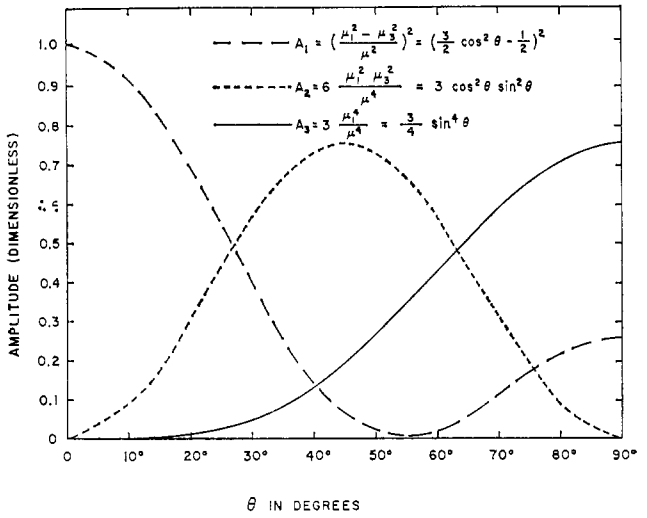

FIGURE 9: Plot of the three amplitudes appearing in eq 1. θ is the angle between the transition dipole of the fluorescent probe and the symmetry axis of the macromolecule.

Theory of Time-Dependent Fluorescence Depolarization. In view of the fact that nanosecond depolarization work on asymmetric macromolecules is only beginning to appear in the literature, we will present a relatively detailed analysis of our depolarization data.

The decay of the polarization anisotropy $r(t) = [I_{\parallel}(t) - I_{\perp}(t)]/[I_{\parallel}(t) + 2I_{\perp}(t)]$ for a fluorescence-labeled macromolecule undergoing Brownian rotational motion depends on the shape and the volume, V, of the macromolecule, the temperature and viscosity of the medium, and the orientation of the label with respect to the macromolecule. In the most general case, when the macromolecule has no symmetry properties at all, five exponentials (Tao, 1969) appear in $r(t)$. Since this is far beyond the resolution of present day experimental methods, one usually has to resort to fitting the data by assuming certain well-defined shapes for the macromolecules. It is particularly convenient to treat the data as if they were true ellipsoids of revolution, because the hydrodynamic properties of such bodies have been worked out in detail. Thus for prolate and oblate ellipsoids, the decay of $r(t)$ is described by three exponentials (Memming, 1961; Wahl, 1966)

$$r(t) = r_0[A_1(\theta)e^{-t/\tau_1} + A_2(\theta)e^{-t/\tau_2} + A_3(\theta)e^{-t/\tau_3}] \quad (1)$$

where r_0 is the intrinsic polarization anisotropy of the fluorescence label and θ is the angle subtended by the transition moment of the label with respect to the symmetry axis of the body

$$A_1(\theta) = \left(\frac{3}{2}\cos^2\theta - \frac{1}{2}\right)^2$$

$$A_2(\theta) = 3\cos^2\theta\sin^2\theta$$

$$A_3(\theta) = \frac{3}{4}\sin^4\theta$$

TABLE III: Rotational Diffusion Relaxation Times Appearing in Equation 1 as a Function of Axial Ratios.[a]

ρ	τ_1/τ_D	τ_2/τ_D	τ_3/τ_D
	Prolate Ellipsoids		
1	1.0000	1.0000	1.0000
2	1.5049	1.3152	0.9543
3	2.3408	1.7276	0.9674
4	3.3956	2.0984	0.9777
5	4.6405	2.4060	0.9842
6	6.0616	2.6548	0.9884
7	7.6505	2.8549	0.9911
8	9.4008	3.0162	0.9930
9	11.3080	3.1472	0.9944
10	13.3680	3.2545	0.9954
15	25.8607	3.5774	0.9979
20	41.8199	3.7280	0.9988
$1/\rho$			
	Oblate Ellipsoids		
1	1.0000	1.0000	1.0000
2	1.1316	1.1701	1.3032
3	1.4645	1.5147	1.6885
4	1.8431	1.9003	2.0955
5	2.2398	2.3018	2.5104
6	2.6455	2.7111	2.9290
7	3.0564	3.1247	3.3495
8	3.4705	3.5411	3.7711
9	3.8869	3.9593	4.1934
10	4.3049	4.3787	4.6162
15	6.4073	6.4859	6.7338
20	8.5193	8.6005	8.8538

[a] ρ is the axial ratio, or ratio of the longitudinal semiaxis to the equatorial semiaxis, $\tau_1 = 1/6D_{\perp}$, $\tau_2 = 1/(5D_{\perp} + D_{\parallel})$, $\tau_3 = 1/(2D_{\perp} + 4D_{\parallel})$, and $\tau_D = 1/6D = V\eta/kT$ is the relaxation time under the spherical model.

τ_1, τ_2, and τ_3 are the three rotational relaxation times characterized by the diffusion coefficients

$$\tau_1 = 1/6D_{\perp}$$

$$\tau_2 = 1/(5D_{\perp} + D_{\parallel})$$

$$\tau_3 = 1/(2D_{\perp} + 4D_{\parallel})$$

$D_{\parallel}$ is the diffusion coefficient for rotation about the symmetry axis, and $D_{\perp}$ is the diffusion coefficient for rotation about an axis that is perpendicular to the symmetry axis of the body.

Perrin's hydrodynamic equations (Perrin, 1936) allow us to calculate $D_{\parallel}$ and $D_{\perp}$, and hence the three relaxation times as a function of the axial ratio ρ between the longitudinal axis and the equatorial axis of the ellipsoid. The values of the relaxation times are tabulated in Table III normalized

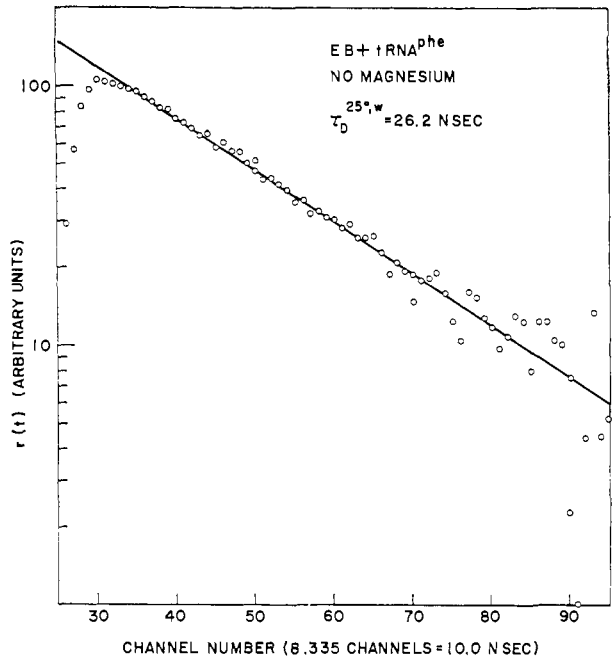

FIGURE 10: Decay of the fluorescence anisotropy of ethidium bromide bound to tRNA^{Phe} in the absence of 0.0026 M magnesium ion. The solid line is a single exponential fit.

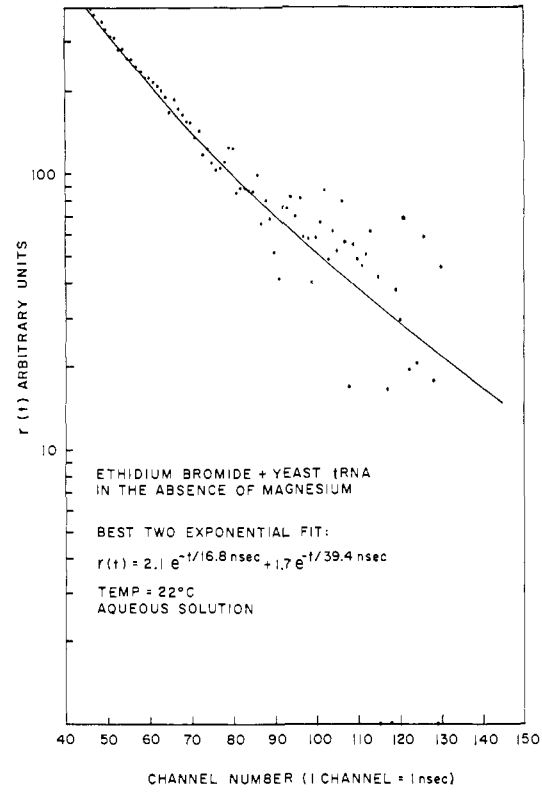

FIGURE 11: Decay of the fluorescence anisotropy of ethidium bromide bound to unfractionated yeast tRNA in the absence of magnesium.

by the relaxation time of an equivolume sphere under the same conditions of temperature, T, and viscosity, η

$$\frac{1}{\tau_D} = \frac{kT}{V\eta} \tag{2}$$

This table is adapted from Tao (1969) as a convenience for the reader.

As is evident, the relaxation behavior according to each of the three relaxation times is weighted by the three coefficients $A_1(\theta)$, $A_2(\theta)$, and $A_3(\theta)$. The values of these coefficients are plotted against the orientation angle, θ, in Figure 9. Table III together with Figure 9 can readily be applied to fluorescence depolarization data and yield structural parameters of macromolecules, as will be demonstrated below.

Nanosecond Depolarization Studies. For most samples, the decay of the EB fluorescence polarization anisotropy, $r(t)$, was a simple exponential (see Figure 10 for a typical example). The slopes of semilogarithmic plots for $r(t)$ yielded the rotational relaxation times, which are tabulated in Table III. Only sample C exhibited a nonexponential anisotropy decay as shown in Figure 11. Two exponentials were used to fit the curve. Note that the two amplitudes are nearly the same.

A single exponential decay of the anisotropy means that to a first approximation the macromolecules may be taken to be spherical in shape, and the relaxation times are simply proportional to the hydrated molecular volume, V, according to the Einstein equation (eq 2). Thus for unfractionated yeast tRNA in the presence of 0.003 M Mg^{2+}, for example, $\tau_D^{25°,w}$ = 24.8 nsec corresponds to a molecular volume V = 114,000 Å^3, or a Stokes' radius r = 30.1 Å. Almost identical results are found for the yeast tRNA^{Phe} samples. These are in quite good agreement with r = 28.5 Å measured by hydrodynamic methods (Adams *et al.*, 1967). It is, however, much larger than the calculated anhydrous volume V_a = 22,200 Å^3 (see Table IV). If this excess was attributed to water of hydration, we would find δ_s = 2.1 g of H_2O/g of tRNA as the extent of hydration. This is astonishingly high, but recent nuclear magnetic resonance work on hydration properties of macromolecules (Kuntz *et al.*, 1969) indicates that such high extents of hydration are not totally implausible for tRNA. For unfractionated yeast tRNA in the presence of magnesium, I. D. Kuntz and J. R. Fresco (private communication) measured δ_s = 1.2 g/g. Assuming this value to be correct, the excess in our δ_s may then be interpreted to indicate a certain amount of elongation in the macromolecule.

As a second approximation we will assume that the tRNA molecule is an ellipsoid of revolution. Equation 1 must now be used to analyze the fluorescence anisotropy. First one calculates the effective hydrated volume of the ellipsoid using the measured value of the hydration cited above. The result is 75,000 Å^3. Our measured effective volume is a factor of 1.52 larger. This excess volume is assumed to arise from the fact that the molecule is nonspherical. It is exactly analogous to the shape factors used in interpreting translation friction coefficients derived from diffusion or sedimentation data.

The complication is that of the three possible relaxation times given in eq 1 only one has been observed. This may correspond to any one of ratios τ_1, τ_2, or τ_3. If the macromole-

TABLE IV: Rotational Relaxation Times[a] and Corresponding Molecular Volumes of tRNAs.

Sample	$\tau_D^{25°,w}$ (nsec)	Vol (Å^3)
A, bulk, 0.04 M Mg^{2+}	31.5	145,000
B, bulk, 0.003 M Mg^{2+}	24.8	114,000
C, bulk, no Mg^{2+}	15.5, 36.4	74,000
D, Phe, 0.0026 M Mg^{2+}	24.5	114,000
E, Phe, no Mg^{2+}	25.2	116,000
Anhydrous bulk yeast[b]		22,200
Hydrated bulk yeast[c]		75,000
Hydrodynamic data[d]		97,200

[a] The relaxation times were corrected to 25° and the viscosity of water at that temperature. [b] Calculated from partial specific volume $\bar{v}$ = 0.503 ml/g (D. D. Henley, T. Lindahl, and J. R. Fresco, unpublished observations quoted by Adams *et al.*, 1967), and molecular weight M = 26,400 g/mole (Lindahl *et al.*, 1965). [c] Using a degree of hydration δ_s = 1.2 g of H_2O/g of tRNA (I. D. Kuntz and J. R. Fresco, private communication). [d] Results of Adams *et al.* (1967) for bulk yeast tRNA.

TABLE V: Range of Axial Ratios for Bulk Yeast tRNA in the Presence of Magnesium.[a]

Assumed δ_s g of H_2O/g of tRNA	Axial Ratio ρ If $\theta \simeq 0°$	Axial Ratio ρ If $\theta \simeq 40°$
2.1	1.0	1.0
1.4	1.8	2.2
1.2	2.0	2.5
1.0	2.3	3.0

[a] θ is the orientation angle between the transition moment of the fluorescent label and the long axis of the assumed prolate ellipsoidal model. See text for details.

cule is assumed to be oblate, the axial ratio would be about 1/3.0 regardless of which relaxation time is taken. This is evident from Table III which shows that for oblate ellipsoids the three relaxation times are comparable in magnitude at all axial ratios. Since an oblate geometry is considered unlikely for tRNAs because of the constraints of the cloverleaf secondary structure, we next consider a prolate geometry. Here we must take into consideration the orientation angle θ between the transition dipole of the dye, and the symmetry axis of the assumed prolate ellipsoid. Since the observed relaxation behavior is a single exponential, we consider only those ranges of θ in which only one of the three amplitudes A_1, A_2, and A_3 dominates. Figure 9 clearly shows that there are only two such ranges of θ: angles around θ = 0°, and θ = 40°. The former corresponds to predominant relaxation according to τ_1, the latter to τ_2. For θ = 0°, the ratio 1.52 corresponds to τ_1/τ_D, and the axial ratio ρ is predicted to be 2.0. Similarly, for θ = 40°, ρ is predicted to be 2.5. It is clear that with so many uncertain variables (notably δ_s and θ), only a range of structural parameters can be given. The variations in ρ depending on δ_s and on θ are shown in Table V. It is evident, nonetheless, that in the presence of magnesium, the tRNAs in the unfractionated sample are only slightly elongated.

For the sample of unfractionated yeast tRNA without magnesium (sample C), the fact that at least two relaxation times were detected immediately rules out a spherical geometry. The ratio of 2.34 between the long and short components of relaxation would give rise to an astronomical axial ratio if the macromolecule resembles an oblate ellipsoid (see Table III). The data must therefore be interpreted in terms of a prolate ellipsoid. The two observed relaxation times may correspond, in principle, to either one of the three combinations: (I) τ_1 and τ_2, (II) τ_1 and τ_3, and (III) τ_2 and τ_3. We think case I is unlikely because only in the region of θ = 90° are both A_1 and A_3 nonzero (see Figure 9). In this region of θ, however, A_3 is about four times as large as A_1, and it was impossible to fit the experimental anisotropy curve with the amplitude of the short relaxation component more than two times as large as that of the long one.

If case II were correct the observed ratios of long and short relaxation times would have to correspond to τ_1/τ_3. Using the data in Table V, one finds the axial ratio to be ρ = 6.1. From this the hydrated molecular volume can be calculated to be 27,000 Å^3. To determine the hydration one now needs an estimate of the anhydrous molecule volume. This can be obtained by using the partial specific volume of $\bar{v}$ = 0.531 ml/g (Henley *et al.*, 1966) and molecular weight M = 26,400 (Lindahl *et al.*, 1965) measured for denatured tRNA in the absence of magnesium. The result is an anhydrous volume of 23,000 Å^3. The extent of hydration is then δ_s = 0.1 g/g. After similar calculations for case III, one finds ρ = 4.6, V = 74,000 Å^3, and δ_s = 1.2 g/g. In view of experimental findings for δ_s we must take this last case as most reasonable. The actual reported value for δ_s is 1.7 g/g (Kuntz *et al.*, 1969) although more recent results suggest δ_s = 1.5 to 1.7 g per g (I. D. Kuntz and J. R. Fresco, private communication). It should be cautioned that in this measurement for sample C, fitting the experimental anisotropy decay curve was rather a trecherous affair, and introduced a good deal of error in the absolute values of the axial ratio and hydration reported here. The very fact that the anisotropy decay curve was nonexponential, however, allows us to conclude that the tRNAs in the unfractionated samples are significantly elongated when magnesium was removed. Our result, an axial ratio of 4.6 is in good agreement with the findings of others. For low magnesium or denatured tRNA samples, the small-angle X-ray-scattering studies of Krigbaum and Godwin (1968) yielded ρ = 3.98, and hydrodynamic work (Kay and Oikawa, 1966; Fresco, 1968) was interpreted as indicating that ρ = 5. These relatively long axial ratios are inconsistent with most of the proposed tertiary structures based on the cloverleaf model. Given the volume and axial ratio found, for example, the short semiaxis is calculated to be 15 Å, and the long semiaxis to be 70 Å. It seems likely that the "denatured" form of tRNAs resemble hairpin structures like those proposed by Brown and Zubay (1960). Probably, these structures could be formed in the absence of magnesium because they tend to minimize the electrostatic

repulsion between the incompletely shielded phosphate groups.

In spite of possible uncertainty about which relaxation time to choose, our results in magnesium are also generally compatible with previous work. Our Stokes' radius in the presence of magnesium, of 30.1 Å is comparable with the value of 28.5 Å obtained from sedimentation and viscometry work (Adams *et al.*, 1967). Small-angle X-ray data under the same conditions (Lake and Beeman, 1968) as interpreted by Krigbaum and Godwin (1968) suggest prolate structures with axial ratios between 1.8 and 3.0, given a hydration of $\delta_s = 1.2 \pm 0.2$ g/g.

It is noteworthy that, like $tRNA^{Phe}$, the decay of the anisotropy for unfractionated yeast tRNA in the presence of magnesium is a single exponential with the same relaxation time. This is taken to indicate that the gross hydrodynamic conformation of most tRNAs in the bulk sample are relatively homogeneous. Thus the use of unfractionated material in our studies and earlier hydrodynamic studies (Adams *et al.*, 1967) is justified so long as the interest lies in the overall gross conformations. On the other hand, it is clear that for many other types of measurements such as optical studies on secondary structure and thermal unfolding studies, it is important to use highly purified samples of tRNA.

Early experiments raised the suspicion that aggregation was occurring in those samples that contained magnesium. Samples were therefore stored overnight at 4° and measurements were retaken. For samples A and B, $\tau_D^{25°,w}$ increased from 31.5 and 24.8 nsec to 41.0 and 28.1 nsec, respectively. In addition, there were small proportions of shorter relaxation time components. No such time-dependent changes in relaxation behavior were observed for sample C (bulk yeast tRNA, no magnesium) or for the $tRNA^{Phe}$ samples. This is consistent with the aggregation studies of Millar and Steiner (1966).

Without accurate molecular weight determinations, the presence of aggregation cannot be positively ruled out. In fact, for those samples containing magnesium such behavior is to be expected (Millar and Steiner, 1966). We believe that the extent of aggregation is small, however, because of the favorable agreement between the molecular volumes found for sample B and that found by Adams *et al.* (1967). Moreover, the results for sample B were comparable with what was found for those samples that are known to be free of aggregation (sample E). In any case, the effect of aggregation would be to reduce the elongation of the tRNAs in sample B.

Additional Conclusions from Nanosecond Depolarization. The results obtained for overall size and shape of tRNA are in good agreement with previously published values. Because of this, a number of important additional conclusions can be drawn from our data. It should be noted that in all calculations we have treated the tRNA molecule as if it were a rigid hydrodynamic particle. This must be true to a large extent, for otherwise one should expect to find much faster relaxation times than what were observed. The rigidity of tRNA probably arises in part from hydrogen bonds between bases not involved in the basic cloverleaf structure. Additional contributions may come from salt linkages such as magnesium ion bridges between phosphates, from the intrinsic difficulty of rotation about bonds in the phosphodiester backbone, and from a base-paired tertiary structure.

For similar reasons one can conclude that the bound EB is rigidly attached to the tRNA. It is also possible to get some information about the orientation of the bound dye. For unfractionated yeast tRNA in the absence of magnesium recall that in the analysis of the depolarization data, we identified τ_2 and τ_3 as the observed relaxation times. An examination of Figure 9 immediately reveals that for both A_2 and A_3 to be substantial concomitantly, the angle θ between the symmetry axis of the body and the transition moment of the dye must be about 63°. Since the optical transition in EB is almost certainly polarized in the plane of the phenanthridinium ring, it seems likely that the flat plane of the intercalated EB and hence the plane of the base pairs is inclined at an angle of 63° to the symmetry axis. This is all quite consistent with the hairpin structure in which the base pairs are tilted at an angle less than 90° from the helix axis. In comparison, in double-stranded and synthetic RNAs the base pairs are tilted 70–80° from the helix axis (Davies, 1967).

The overall success of these first attempts at fluorescence lifetime and nanosecond depolarization measurements on nucleic acids is very encouraging. Considerable additional information can be obtained on tRNA structure if the fluorescence of groups covalently attached to the tRNA is examined. A number of such studies are currently in progress in our laboratory. The fluorescence of ethidium bromide, noncovalently bound to nucleic acids should be a useful tool for examining the structure of other nucleic acids such as r- and mRNAs. It should also be possible to extend the approaches described herein to the study of complexes between proteins and nucleic acids. As information on more complicated systems is sought, the advantages of these fluorescence techniques will become increasingly apparent.

Acknowledgment

We are grateful to Professor Richard Bersohn in whose fluorescence laboratory the bulk of this work was conducted. We appreciated and enjoyed many helpful discussions with Mr. Kenneth Beardsley, Mr. Robert Dichter, and Mr. Chung K. Luk. Ethidium bromide was a gift from the Boots Pure Drug Co., Ltd., Nottingham, England. Several preliminary experiments on the binding of ethidium bromide to unfractionated yeast tRNA were performed by Mrs. Marta Ventilla. We thank Professor Irwin D. Kuntz and Professor Jacques R. Fresco for permitting us to cite some of their unpublished results and for very helpful discussions.

References

Adams, A., Lindahl, T., and Fresco, J. R. (1967), *Proc. Nat. Acad. Sci. U. S. 57*, 1684.

Beardsley, K., and Cantor, C. R. (1970), *Proc. Nat. Acad. Sci. U. S. 65*, 39.

Beardsley, K., Tao, T., and Cantor, C. R. (1970), *Biochemistry 9*, 3524.

Bittman, R. (1969), *J. Mol. Biol. 46*, 251.

Brown, G. L., and Zubay, G. (1960), *J. Mol. Biol. 2*, 287.

Cantor, C. R., Fairclough, R. H., and Newmark, R. A. (1969), *Biochemistry 8*, 3610.

Cantor, C. R., Jaskunas, S. R., and Tinoco, I., Jr. (1966), *J. Mol. Biol. 20*, 39.

Churchich, J. E. (1963), *Biochim. Biophys. Acta 75*, 274.
Cramer, F., Doepner, H., von der Haar, F., Schlimme, E., and Seidel, H. (1968), *Proc. Nat. Acad. Sci. U. S. 61*, 1384.
Davies, D. (1967), *Annu. Rev. Biochem. 36*, 321.
Fresco, J. R. (1968), *Miles Symp. Trans. Genet. Info. Protein Syn.*, 5.
Fuller, W., and Waring, M. J. (1964), *Ber. Bunsenges. Phys. Chem. 68*, 805.
Haugland, R. P., Yguerabide, J., and Stryer, L. (1969), *Proc. Nat. Acad. Sci. U. S. 63*, 23.
Henley, D. H., Lindahl, T., and Fresco, J. R. (1966), *Proc. Nat. Acad. Sci. U. S. 55*, 191.
Kay, C. N., and Oikawa, K. (1966), *Biochemistry 5*, 213.
Kuntz, I. D., Brassfield, T. S., Law, G. D., and Purcell, G. V. (1969), *Science 163*, 1329.
Krigbaum, W. R., and Godwin, R. W. (1968), *Macromolecules 1*, 375.
Lake, J. A., and Beeman, W. W. (1968), *J. Mol. Biol. 31*, 115.
LePecq, J. B., and Paoletti, C. (1967), *J. Mol. Biol. 27*, 87.
Li, H. J., and Crothers, D. M. (1969), *J. Mol. Biol. 39*, 461.
Lindahl, T., Adams, A., and Fresco, J. R. (1966), *Proc. Nat. Acad. Sci. U. S. 55*, 941.
Lindahl, T., Henley, D. D., and Fresco, J. R. (1965), *J. Amer. Chem. Soc. 87*, 4961.
Madison, J. T. (1968), *Annu. Rev. Biochem. 37*, 131.
Memming, R. (1961), *Z. Phys. Chem. (Leipzig) 28*, 169.
Millar, D. B., and Steiner, R. F. (1966), *Biochemistry 5*, 2289.
Ninio, J., Favre, A., and Yaniv, M. (1969), *Nature (London) 223*, 1333.
Penniston, J. T., and Doty, P. (1963), *Biopolymers 1*, 145.
Perrin, F. (1936), *J. Phys. Radium 7*, 1.
RajBhandary, U. L., Chang, S. H., Stuart, A., Faulkner, R. D., Hoskinson, R. M., and Khorana, H. G. (1967), *Proc. Nat. Acad. Sci. U. S. 57*, 251.
Reeves, R. H., Cantor, C. R., and Chambers, R. W. (1970), *Biochemistry* (in press).
Stryer, L. (1968), *Science 162*, 526.
Stryer, L., and Haugland, R. P. (1967), *Proc. Nat. Acad. Sci. U. S. 58*, 719.
Tao, T. (1969), *Biopolymers 8*, 609.
Thiebe, R., and Zachau, H. G. (1968), *Eur. J. Biochem. 5*, 546.
Wahl, P. (1966), *C. R. Acad. Sci., Ser. D 263*, 1525.
Wahl, P., and Timasheff, S. N. (1969), *Biochemistry 8*, 2945.
Weber, G., and Laurence, D. J. R. (1954), *Biochem. J. 56*, 31p.

Studies on the Conformation of the Anticodon Loop of Phenylalanine Transfer Ribonucleic Acid. Effect of Environment on the Fluorescence of the Y Base*

Kenneth Beardsley,† Terence Tao,‡ and Charles R. Cantor§

ABSTRACT: The fluorescence intensity of the Y base of yeast and wheat germ $tRNA^{Phe}$ is enhanced two- to threefold when magnesium ion is added to a neutral aqueous solution of the tRNA. In 0.1 M NaCl, the range of magnesium concentrations used, 10^{-1} to 10^{-5} M, appears to have little effect on the overall structure of these two tRNA species. Our results suggest, however, that magnesium does have a profound effect on the conformations at or near the anticodon loop. The activity of magnesium is unlikely to be the result of direct binding near the Y base since the fluorescence of a hexanucleotide containing Y is independent of magnesium. The fluorescence lifetime and intensity in this oligomer are considerably less than what was found for magnesium-free tRNA. The fluorescence of $tRNA^{Phe}$ in the absence of magnesium is enhanced by D_2O. A similar enhancement occurs in the hexanucleotide but virtually no effect is observed with intact $tRNA^{Phe}$ when magnesium is present at high concentrations. Studies of the nanosecond depolarization of Y in $tRNA^{Phe}$ show that the fluorescent base is not rigidly attached to the bulk of the tRNA. The fluorescence is partially depolarized both in the presence and absence of magnesium. All of these results are consistent with the following picture. The Y base is quenched by contact with water. When magnesium is present, the conformation of $tRNA^{Phe}$ changes in such a way that the Y base is shielded from the solvent.

Most physical techniques that have been used to study the conformation of tRNA provide information about the average secondary structure or overall shape (Cantor *et al.*, 1966; Englander and Englander, 1965; Adams *et al.*, 1967; Lake and Beeman, 1968). To construct an accurate picture of the structure of tRNA in aqueous solution it is necessary to obtain detailed information about the relative stability and proximity of a number of important regions of the

* From the Departments of Chemistry and Biological Sciences, Columbia University, New York, New York 10027. *Received December 12, 1969.* Supported by grants from the National Institutes of Health (GM 14825 to C. R. C. and CA 07712 to Professor Richard Bersohn).
† Supported by U. S. Public Health Service Training Grant No. 5T0-1-GM01130.

‡ Present address: Department of Molecular Biophysics, Yale University.
§ Alfred P. Sloan Fellow.